In–flight effective area calibration of the Chandra low energy transmission grating spectrometer

Deron Pease[1], Jeremy J. Drake[1], Vinay Kashyap[1], Herman L. Marshall[2], Erica L. Raffauf[1], Peter W. Ratzlaff[1], Bradford J. Wargelin[1]

[1] *Smithsonian Astrophysical Observatory, 60 Garden Street, Cambridge, MA, USA 02138*

[2] *Center for Space Research, M.I.T., Cambridge, MA, USA 02139*

Abstract

We present the in-flight effective area calibration of the Low Energy Transmission Grating Spectrometer (LETGS), which comprises the High Resolution Camera Spectroscopic readout (HRC-S) and the Low Energy Transmission Grating (LETG) aboard the *Chandra X-ray Observatory*. Previous studies of the LETGS effective area calibration have focused on specific energy regimes: 1) the low-energy calibration for which we compared observations of Sirius B and HZ 43 with pure hydrogen non-LTE white dwarf emission models; and 2) the mid-energy calibration for which we compared observations of the active galactic nuclei PKS 2155−304 and 3C 273 with simple power-law models of their seemingly featureless continua. The residuals of the model comparisons were taken to be true residuals in the HRC-S quantum efficiency (QE) model. Additional in-flight observations of celestial sources with well-understood X-ray spectra have served to verify and fine-tune the calibration. Thus, from these studies we have derived corrections to the HRC-S QE to match the predicted and observed spectra over the full practical energy range of the LETGS. Furthermore, from pre-flight laboratory flatfield data we have constructed an HRC-S quantum efficiency uniformity (QEU) model. Application of the QEU to our semi-empirical in-flight HRC-S QE has resulted in an improved HRC-S on-axis QE. Implementation of the HRC-S QEU with the on-axis QE now allows for the computation of effective area for any reasonable *Chandra*/LETGS pointing.

Targets & Models

Table 1: Summary LETG+HRC-S Calibration Observations

Target	Obs ID	Date	Exposure (s)	Status[a]
Sirius B	1452	1999-10-26	27527	primary
	1459	1999-10-27	11909	primary
	1421	1999-10-28	24706	primary
HZ 43	59	1999-11-12	39798	secondary
	1011	2001-05-18	18653	secondary
	1012	2001-08-18	19947	secondary
	2584	2002-01-01	19003	secondary
PKS 2155−304	331	1999-12-25	62658	primary
	1704	2000-05-31	25835	secondary
	1013	2001-04-06	26643	secondary
	3166	2001-11-30	29771	secondary
3C 273	460	2000-01-09	39939	secondary
RX J1856.5−3754	113	2000-03-10	55121	secondary
	3382	2001-10-08	101172	secondary
	3380	2001-10-10	166325	secondary
	3381	2001-10-12	169956	secondary
	3399	2001-10-15	9282	secondary

[a] Status column indicates whether observation was employed to make the semi-empirical corrections to HRC-S QE (primary) or to monitor/fine-tune the effective area (secondary)

Source Parameters

Mid-E Cal
0.28–2.0 keV, 6–44 Å

Low-E Cal
0.06–0.28 keV, 44–200 Å

Blazar **PKS 2155−304**
- Single power-law
- $\Gamma \approx 2.45$, $N_{\rm H} = 1.36 \times 10^{20}$ cm^{-2}

WD **Sirius B**
- Pure hydrogen non-LTE emission producing featureless continua
- $T_{\rm eff} = 25000$ K & $\log g = 9.0$

Quasar **3C 273**
- Broken power-law
- $\Gamma_1 = 1.56, \Gamma_2 = 2.1$, $N_{\rm H} = 1.71 \times 10^{20}$ cm^{-2}

WD **HZ43**
- $T_{\rm eff} = 51000$ K & $\log g = 7.9$

Compact object **RX J1856.5−3754**
- ~ 60 eV (7×10^5 K) blackbody
- 8×10^{19} cm$^{-2} \le N_{\rm H} \le 1.1 \times 10^{20}$ cm^{-2}

Initial Comparison

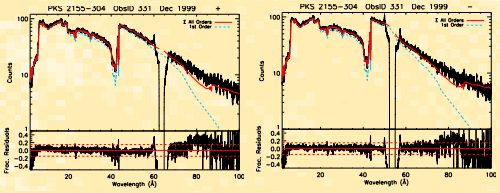

Comparison of the pre-correction model-predicted spectrum for PKS 2155−304 with the observed LETGS spectrum (ObsID 331) illustrates inadequacies in the model (see large fluctuations in the residuals), which we attribute to errors in the HRC-S QE. Dashed lines on residuals plots are 15% error lines. Positive (left) and negative (right) orders are plotted separately. Data have been smoothed by 10 pixels (1 pixel = 0.0125 Å).

Correction Methodology

$A_{\rm eff:\ LETG} = A_{\rm eff:\ HRMA} \times \Phi_{\rm LETG} \times T_{\rm UVIS} \times Q_{\rm HRC-S\ MCP}$

- Comparison of PKS 2155−304 model to observed spectrum indicates problems in QE
  - higher energy mismatch over $\sim 1-6$ keV (2–12 Å)
  - Cs-M$_{\rm IV,V}$ edges near ~ 0.74 keV (16.8 Å)
  - a misalignment of the C-Kα edge ~ 0.28 keV (44 Å)
  - mid-to-low mismatch over $\sim 0.18-0.15$ keV (70–80 Å)
- Derive corrections from ratio of data to model
- -0.25 eV shift UV/ion shield transmission model required
- Apply correction to HRC-S QE
- Test: compare new model with more observations (PKS 2155−304 & 3C 273) and find good agreement
- Positve/Negative LETG dispersion orders treated separately

QE Uniformity & On-Axis QE

- Construct QEU map from lab flatfield data
- Apply QEU to derive improved on-axis QE
- Compute LETGS effective areas

QE Correction Curves

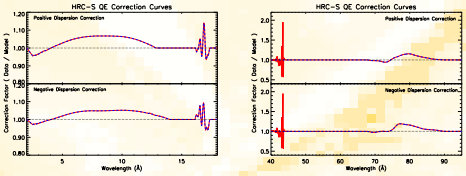

HRC-S QE fine-tuning correction curves derived from in-flight calibration using primarily PKS 2155−304 (ObsID 331). The left plot shows corrections to the high energy mismatch and the Cs-M edges. The right plot shows the HRC-S UV/ion shield shift and the smoothing of the MCP QE mid-to-low calibration joining region. Positive and negative dispersion corrections are shown separately.

Correction Confirmation

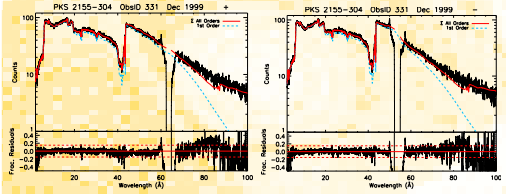

Details

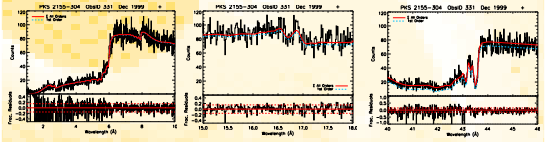

Details of the energy regimes of interest. The left plot shows the repaired higher energy mismatch over $\sim 1-6$ keV (2–12 Å). The middle plot shows the inclusion of the Cs-M$_{\rm IV,V}$ edges near ~ 0.74 keV (16.8 Å). The right plot shows the improved alignment of the C-Kα edge ~ 0.28 keV (44 Å). Note the remaining mismatch at ~ 43 Å. Dashed lines on residuals plots are 15% error lines. Data have been binned by CIAO pixel size (0.0125 Å). Only data from positive dispersion are shown. Negative dispersion corrections display similar results.

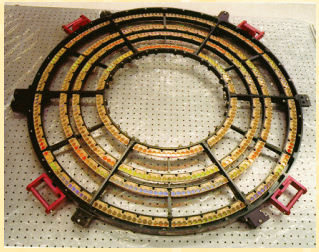

Good agreement with more observations

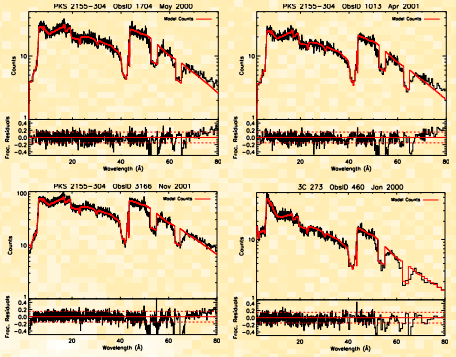

Post-correction model prediction compared with the May 2000 observation of PKS 2155−304, $\Gamma = 2.42$ (top left); April 2001 observation of PKS 2155−304, $\Gamma = 2.38$ (top right); November 2001 observation of PKS 2155−304, $\Gamma = 2.45$ (bottom left); and January 2000 observation of 3C 273, $\Gamma_1 = 1.56$, $\Gamma_2 = 2.1$ (bottom right). Positive and negative orders have been combined and the spectra have been adaptively binned to signal-to-noise of 7.5. Dashed lines on residuals plots are 15% error lines. Modeled gaps do not include the effects of dither.

QEU & On–axis QE

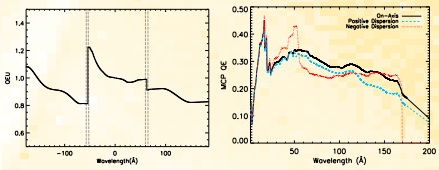

Left plot shows HRC-S QE uniformity curve for a rectangular strip located within the LETG nominal extraction region. Wavelength is paired with LETG dispersion location unique to photon energy. The vertical dotted lines indicate plate boundaries. Right plot shows the new, post-correction on-axis MCP QE shown along with the MCP QEs which follow positive and negative LETG dispersions. This figure also serves to illustrate the effects of the non-uniformity of the MCP QE.

Corrected effective area model orders 0–3, full active range

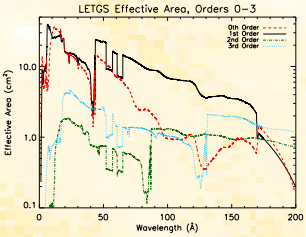

Caveats

Highly accurate calibration from in-flight data is difficult:

- Separation of individual model components from total throughput model (ex. HRC-S MCP QE from UV/ion shield transmission)
- Heavily source model dependent: Is PKS 2155-304 really best modeled by single P-L?
- Complex high order separation & diffraction efficiencies uncertainties
- Errors subsumed by HRC-S MCP QE

Conclusions

- Present the full-range LETGS Effective Area calibrated from in-flight data
- Made minor but important adjustment to UV/ion shield transmission model
- Constructed QEU map & derived on-axis QE
- Implementation of HRC-S QEU with on-axis QE allows computation of effective area for any reasonable *Chandra*/LETGS pointing
- Continue to monitor and fine-tune low-E response with HZ 43, and mid-E response with PKS 2155−304, 3C 273 & RX J1856.5−3754
- Even though difficult from in-flight data, we've produced an accurate calibration

http://asc.harvard.edu/cal/Links/Letg/User